NMR Studies of the Dynamics of the Multidomain Protein Urokinase-type Plasminogen Activator†

Ursula K. Nowak,‡ Xiang Li,‡ Andrew J. Teuten,‡ Richard A. G. Smith,§ and Christopher M. Dobson*,‡

Oxford Centre for Molecular Sciences and Inorganic Chemistry Laboratory, University of Oxford, South Parks Road, Oxford OX1 3QR, U.K., and SmithKline Beecham Pharmaceuticals, Yew Tree Bottom Road, Great Burgh, Epsom, Surrey KT18 5XQ, U.K.

Received July 28, 1992; Revised Manuscript Received October 26, 1992

ABSTRACT: u-PA (urokinase-type plasminogen activator or urokinase) has been studied under a variety of solution conditions by 1-D and 2-D NMR spectroscopy. Very high quality spectra could be obtained from the recombinant protein despite the high molecular mass (46 kDa) by appropriate choice of solution conditions; mildly acidic pH and low ionic strength were found to be optimal. Comparison of spectra of u-PA with spectra of the isolated kringle and protease domains, the EGF–kringle pair, and a synthetic peptide from the kringle-protease linker region, enabled sequential assignments in the u-PA spectrum to be made for kringle resonances, and domain-specific assignments for many others. Simulations of line shapes in both 1-D and 2-D spectra enabled effective correlation times for the different domains, both isolated and in the intact protein, to be determined. These have permitted a model of the u-PA dynamics to be put forward involving extensive, but not unrestricted, motion between the different domains.

u-PA[1] (urokinase-type plasminogen activator, urokinase) is a member of the family of multidomain fibrinolytic proteins and, together with t-PA (tissue plasminogen activator), is one of the major activators of plasminogen. Although the biological role of t-PA is almost solely concerned with the dissolution of blood clots, u-PA has also been found to be important in a number of other processes. Its involvement in processes of tissue degradation has suggested a role for u-PA in the invasiveness of tumors and the process of metastasis (Dano et al., 1985). u-PA has been investigated as a new prognostic marker in cancer, as its level in primary cancers is related to the metastatic potential (Reilly et al., 1991).

u-PA is synthesized in the kidney and can be isolated from plasma, urine, and certain cancer cell cultures. It is secreted as a 54-kDa single-chain glycoprotein (scu-PA or pro-urokinase) which shows some properties of a protease zymogen, such as the lack of reactivity with protease inhibitors (Gurewich et al., 1984) and peptide–chloromethylketone derivatives (Lijnen et al., 1987). It does, however, possess some, albeit low, intrinsic catalytic activity (Gurewich et al., 1988; Lijnen et al., 1990). scu-PA is activated to the fully active two-chain form by cleavage between the Lys-158 and Ile-159 bond by plasmin (Holmes et al., 1985); the two chains remain connected by a disulfide bridge. Recombinant scu-PA has been expressed in *Escherichia coli* (Winkler et al., 1985; Winkler et al., 1986; Holmes et al., 1985) and has a molecular mass of 46 kDa, reduced from that of the native protein by the absence of carbohydrate; u-PA of urinary origin has a glycosylation site at Asn-302 (Steffens et al., 1982). Recombinant u-PA has been shown to have similar functional properties to u-PA isolated from human urine (Günzler et al., 1984).

Three different domains can be distinguished in the sequence of u-PA: the N-terminal epidermal growth factor like (EGF-like) domain, the kringle domain, and the C-terminal proteolytic domain. These domains have significant homology with domains found in other proteins and are probably related in evolution (Gilbert, 1978; Patthy, 1985). The EGF-like domain (residues 5–45, 5 kDa) is related to human epidermal growth factor and binds to the u-PA receptor (Appella et al., 1987; Blasi et al., 1988). The functional role of the kringle domain (residues 46–135, 10 kDa) remains unclear, although is has been shown that the kringle domain of u-PA binds heparin and might also bind to cell-surface polyanions (Stephens et al., 1992). It does not exhibit the fibrin binding specificity found in other homologous domains, such as kringle 1 and 4 in plasminogen and kringle 2 in t-PA. The third domain is a trypsin-like serine protease domain (residues 136–411, 33 kDa), which contains the "catalytic triad" (His-204, Asp-255, and Ser-356) found in all serine proteases (Steffens et al., 1982). It is connected to the kringle domain by a 16-residue long linker peptide and can be isolated following cleavage at Lys-135 during limited proteolysis by plasmin. The resulting low molecular weight u-PA (LMW u-PA) is fully active and is also present in body fluids. Activation of scu-PA to two-chain u-PA (tcu-PA) by cleavage at Lys-158 leads to a new amino terminus which might form an ion pair with Asp-355 by intruding into the proteolytic domain in the manner found for other serine proteases (de Munk & Rijken, 1990).

At the present time little is known about the physical and structural properties of intact u-PA. The protein has a high content of β-sheet and β-turn secondary structure, as seen in CD studies (Mangel et al., 1991). In common with other multidomain proteins, crystallization conditions have proved elusive, and there is no crystal structure presently available. Investigation by small-angle neutron scattering has indicated a highly asymmetric molecule with a radius of gyration of 31 Å and a maximum dimension of 90 Å (Mangel et al., 1991). Although u-PA is large in respect to its feasibility for NMR

† This is a contribution from the Oxford Centre for Molecular Sciences, which is supported by the Science and Engineering Research Council and the Medical Research Council of the United Kingdom. U.K.N. was supported by the European Science Exchange Programme funded by the Royal Society and the Österreichischen Akademie der Wissenschaften.

* Author to whom correspondence should be addressed.

‡ University of Oxford.

§ SmithKline Beecham Pharmaceuticals.

[1] Abbreviations: NMR, nuclear magnetic resonance; DQF COSY, double-quantum-filtered correlated spectroscopy; TOCSY, total correlated spectroscopy; u-PA, urokinase-type plasminogen activator; EGF, epidermal growth factor; 1-D, one dimensional; 2-D, two dimensional.

0006-2960/93/0432-298$04.00/0

studies, important information has been gained from preliminary NMR studies on this protein (Oswald et al., 1989; Bogusky et al.,1989). Comparison of spectra of the intact protein with those of the isolated domains provided evidence for close structural similarity between the isolated domains and the corresponding units of the intact protein. Furthermore, these studies showed that the domains have a substantial degree of structural independence in terms of both their dynamical behavior and their folding properties. Indeed, it is to these properties that the feasibility of NMR studies is attributed (Oswald et al., 1989).

As with other multidomain proteins, one approach to structural analysis has been to isolate individual domains and to investigate their structures. The kringle domain of u-PA which can be isolated by extended plasminolysis (Bogusky et al., 1989; Mazar et al., 1992) has been studied by NMR (Li et al., 1992), and its secondary structure elements have been determined. These include three antiparallel β-sheets, two helices, and three tight β-turns. One of the helices is analogous to that reported for t-PA kringle 2 (Byeon et al., 1991; de Vos et al., 1992), but the other one is so far unique to the u-PA kringle. The overall tertiary fold has at present been determined only in outline but is similar to the crystal structures of prothrombin kringle 1 (Park & Tulinsky, 1986; Tulinsky et al., 1988), plasminogen kringle 4 (Mulichak et al., 1991; Wu et al., 1991), and especially t-PA kringle 2 (de Vos et al., 1992; Byeon & Llinás, 1991).

In this paper we extend considerably previous NMR studies of u-PA and its component domains and investigate a peptide synthesized to correspond to the linker region between the kringle and the protease domain (residues 136–158). Much improved NMR spectra were achieved by the use of recombinant protein and careful optimization of conditions, and these have enabled us to analyze 1-D and 2-D spectra in some detail. In particular, the nature of domain mobility within u-PA has been investigated by simulating 1-D and 2-D spectra to obtain information about the overall motional correlation times for the domains, and these data have enabled us to put forward a dynamical model for this multidomain protein.

MATERIALS AND METHODS

Protein Samples. Recombinant two-chain u-PA, low molecular weight u-PA, and the isolated kringle domain were provided by Grünenthal GmbH, Aachen, Germany. These were derived from single-chain u-PA expressed in *E. coli*, the two-chain protein and fragments being produced by proteolytic cleavage. The recombinant EGF–kringle domain was provided by Dr. D. J. Ballance, Delta Biotechnology Ltd., Nottingham, U.K., and was secreted from the yeast *Saccharomyces cerevisiae*. Human high molecular weight u-PA of urinary origin was a gift of the Japan Chemical Research Co. Ltd., Japan.

Human urinary and recombinant two-chain u-PA and low molecular weight u-PA were prepared in a 0.1 M Tris, 0.15 M NaCl, and 20% (v/v) glycerol containing buffer at pH 7.4 at a concentration of 10 mg/mL and inactivated with a threefold molar excess of GGACK (L-Glu-L-Gly-L-Arg-chloromethylketone, Cambridge Bioscience, Cambridge, U.K.) (20 mM in ethanol) at 25 °C until the activity against S-2444 was reduced to less than 0.5% of that of the untreated protein. Inactivation was carried out to reduce the possibility of autolysis in the NMR experiments during data acquisition, although this is unlikely to be fast at the pH values used in the experiment. The samples were buffer exchanged into 0.1 M NH_4HCO_3 at pH 8.5 on Sephadex G-25M (PD-10, Pharmacia) gel filtration columns at 4 °C and lyophilized.

Inactivated human urinary u-PA was purified on an FPLC system using a gel filtration column (Sephacryl S-100 HiLoad column). A 0.1 M solution of NH_4HCO_3, pH 8.4, was used as the eluting buffer to make direct lyophilization possible. Fractions containing u-PA were pooled after their purity had been confirmed by SDS gel electrophoresis and then lyophilized.

The linker peptide from Lys-136, the cleavage site between the kringle and the protease domain, to Lys-158, the activation site of the protease domain, was synthesized on an automated peptide synthesizer using a *p*-alkoxybenzylalcohol resin and standard Fmoc protocols. The peptide was cleaved from the resin using 90% TFA/5% H_2O/2.5% 1,2-ethanediol/2.5% anisole and was purified by reverse-phase HPLC.

All protein samples were dissolved in D_2O or H_2O at pH 4.5 and purified from small molecule impurities and salts by five cycles of centrifugation at 4 °C (reducing the volume from 2.0 mL to about 150 μL in each step; 4000*g*) using Centricon-3 or Centricon-10 concentration cells with a 3- or 10-kDa cut-off membrane, respectively (Amicon, Gloucester, U.K.). The pH was adjusted by adding dilute DCl and NaOD (2% and 0.2%), and pH values quoted are uncorrected for isotope effects. Sample concentrations were between 0.6 and 2.2 mM.

NMR Spectroscopy. NMR spectra were recorded on a Bruker AM600 spectrometer with a proton resonant frequency of 600.13 MHz at the Oxford Centre for Molecular Sciences. Spectra were collected at 29 or 35 °C. 1-D spectra were recorded using 4K or 8K data points over a spectral width of 7812.5 or 8928.5 Hz, collecting 300–1600 scans. Resolution enhancement was achieved using the Lorentzian–Gaussian transformation (GB 0.15, LB −10) prior to zero-filling to 8K. DQF COSY (Rance et al., 1983) and TOCSY spectra (Braunschweiler & Ernst, 1983; Davis & Bax, 1985) were acquired over 2K data points and 512–800 t_1 increments in the absorption mode with time-proportional phase incrementation (TPPI) for quadrature detection in the t_1 dimension. Water saturation was achieved by low-power irradiation during the relaxation delay introduced between scans. A total of 80, 96 or 112 transients were collected for each t_1 increment. TOCSY spectra were acquired in reverse mode using a MLEV17 pulse sequence (Bax & Davis, 1985) for mixing (mixing time, 47 ms). 2-D spectra were processed on a Sun 4/110 workstation using the Felix program provided by Dr. D. R. Hare (Felix version 1.1, Hare Research Inc.). The data set was resolution enhanced by double-exponential and trapezoidal multiplication in t_2 and a combination of double-exponential, shifted sine-bell-squared and trapezoidal multiplication in t_1 prior to zero-filling in both dimensions. After zero-filling, the digital resolution was 3.8–4.2 Hz/pt in both dimensions. All spectra were referenced to 1,4-dioxane at 3.74 ppm.

Simulations. Spectral simulations for both 1-D and 2-D NMR spectra were performed on a Sun 4 workstation. Simulations of 2-D COSY spectra were carried out using a program provided by Dr. C. Redfield which assumes weak coupling for neighboring protons and applies experimental parameters (line width, coupling, and resolution enhancement functions) to in-phase and antiphase peaks. Tryptophan cross peaks were simulated with the known values of coupling constants ($^3J_{45}$ = 8.03, $^3J_{56}$ = 7.08, $^3J_{67}$ = 8.34, $^4J_{46}$ = 1.12, $^4J_{47}$ = 0.95, $^5J_{47}$ = 0.81) (Redfield, 1984) and varying line width values. The same resolution enhancement functions

were used for the simulations and for processing the NMR data sets (see above). Positive and negative contours of the cross peaks are plotted at exponentially increasing levels.

In order to simulate a tryptophan cross peak, a first estimate of the resonance line width was obtained by determination of the line width of a resolved tryptophan resonance in the 1-D spectrum. A best fit of an experimental 1-D peak to a simulated in-phase signal was made by visual comparison, and then 2-D cross peaks of the same line width were simulated. By adjusting the contour level, the contour profile of the simulated cross peak was compared with the experimental cross peak for a given line width until the two were closely matched. This was then repeated for other cross peaks for the same contour level but different line width values. In addition to visual comparison of the simulated and the experimental cross peaks, the peak heights of the cross peaks were compared. These were measured within the Felix routine, and the four absolute intensities of the maxima and minima of a crosspeak were averaged.

The half-height line width ($\Delta\nu_{1/2}$) for a Lorentzian line is

$$\Delta\nu_{1/2} = \frac{1}{\pi T_2} = \frac{1}{20\pi}\sum[5J(0) + 9J(\omega) + 6J(2\omega)] \quad (1)$$

where T_2 is the transverse relaxation time, and the summation is over all pairwise contributions to the specific spin resonance. Using the formalism of Lipari and Szabo (1982) to account for internal motions, the spectral density function $J(\omega)$ can be written as

$$J(\omega) = \left(\frac{\mu_0\gamma^2\hbar}{4\pi r^3}\right)^2\left[\frac{S^2\tau_c}{1 + (\omega\tau_c)^2} + (1 - S^2)\frac{\tau}{1 + (\omega\tau)^2}\right] \quad (2)$$

where τ_c is the overall rotational correlation time, $\tau^{-1} = \tau_c^{-1} + \tau_{in}^{-1}$, and τ_{in} is the correlation time for internal motions. S^2 is a generalized order parameter, r is the interproton distance, and the other symbols have their conventional meaning. Provided that $\tau_{in} \ll \tau_c$ and $\omega^2\tau_c\tau_{in} \ll 1$, eq 2 can be simplified as

$$J(\omega) = \left(\frac{\mu_0\gamma^2\hbar}{4\pi r^3}\right)^2\frac{S^2\tau_c}{1 + (\omega\tau_c)^2} \quad (3)$$

Taking eq 3 into eq 1 and neglecting contributions from nonlinear terms ($\omega^2\tau_c^2 \gg 1$), we have

$$\Delta\nu_{1/2} = \frac{\tau_{eff}}{4\pi}\sum\left(\frac{\mu_0\gamma^2\hbar}{4\pi r^3}\right)^2 \quad (4)$$

and

$$\tau_{eff} = S^2\tau_c \quad (5)$$

Equation 4 demonstrates that this is a direct proportional relationship between line width and correlation time. For transverse relaxation rates, and hence $\Delta\nu_{1/2}$, where the contribution from $J(0)$ dominates, the errors introduced by the above simplifications will be minimal.

In the absence of structural data for u-PA, an average value for $\sum 1/r^6$ was calculated for the protons of the six tryptophan residues in hen egg white lysozyme from the tetragonal crystal structure data (Handoll, 1985). This was found to be 0.02 $\pm$ 0.005 Å^{-6} and was used for the estimation of τ_{eff} values for u-PA and its fragments.

Simulations were also carried out for methyl group resonances in 1-D spectra. It has long been known that the relaxation processes for methyl protons are complicated by cross-correlation effects (Hubbard, 1958a,b, 1969). The transverse relaxation of an A_3 spin system can be described by using Redfield relaxation matrix theory (Redfield, 1965) or by solving a group of first-order differential equations by forming a set of "normal mode variables" (Werbelow & Marshall, 1973; Werbelow & Grant, 1977). For the latter case, the equations have the form

$$-\frac{d}{dt}\mathbf{q} = \mathbf{R}\cdot\mathbf{q} \quad (6)$$

where $\mathbf{q} = (q_1,q_2,q_3)^T$ is a set of three variables related to transverse coherences, and at least one of them, e.g., q_1, corresponds to the observable transverse magnetization I_x. The matrix elements R_{mn} (m,n = 1,3) are each a linear combination of spectral density functions $J_{ijkl}(\lambda\omega)$ which can be approximated as:

$$J_{ijkl}(\lambda\omega) = \frac{3}{10}\left(\frac{\mu_0\gamma^2\hbar}{4\pi r^3}\right)^2\left[\frac{1}{4}\frac{S^2\tau_c}{1 + (\lambda\omega\tau_c)^2} + \frac{3}{4}\cos(\Omega_{ijkl})\frac{S^2\tau'}{1 + (\lambda\omega\tau')^2}\right] \quad (7)$$

where $\tau'^{-1} = \tau_c^{-1} + \tau_{me}^{-1}$, and τ_{me} is the correlation time for methyl internal motion. In the autocorrelation case, Ω_{ijkl} = 0 and $J_a(\lambda\omega) = J_{ijij}(\lambda\omega)$; in the cross-correlation case, Ω_{ijkl} = $2\pi/3$ and $J_c(\lambda\omega) = J_{ijkl}(\lambda\omega)$.

In practice, ^{1}H methyl relaxation processes are dominated by contributions from external protons. The contribution from each external proton can be calculated using Tropp's model (Tropp, 1980), which gives, for a sphere

$$J(\lambda\omega) = \frac{1}{5}\left(\frac{\mu_0\gamma^2\hbar}{4\pi}\right)^2\sum_{n=-2}^{2}\left[\frac{S^2\tau_c f(n)}{1 + (\lambda\omega\tau_c)^2} + \frac{S^2\tau' g(n)}{1 + (\lambda\omega\tau')^2}\right] \quad (8)$$

with the following definitions:

$$f(n) = \left|\sum_{i=1}^{3}\frac{Y_{2,n}(\Omega_i)}{3r_i^3}\right|^2 \quad (9)$$

$$g(n) = \frac{1}{3}\left|\sum_{i=1}^{3}\frac{Y_{2,n}(\Omega_i)}{r_i^3}\right|^2 - f(n) \quad (10)$$

where $Y_{2,n}$ are second-order spherical harmonics, r_i is the distance between a methyl proton and an external proton, and Ω_i are Euler angles of interproton vectors with respect to the symmetry axis of the methyl group. It should be noted that eq 8 takes account of additional internal motions other than the fast methyl rotations (e.g., side-chain mobilities) and has been simplified by arguments similar to those used in obtaining eq 3. It can be further simplified to give

$$J(\lambda\omega) = \frac{1}{5}\left(\frac{\mu_0\gamma^2\hbar}{4\pi}\right)^2\sum_{n=-2}^{2}\frac{\tau_{eff} f(n)}{1 + (\lambda\omega\tau_c)^2} \quad (11)$$

Solution of eq 6 can be accomplished by using matrix manipulation to give

$$\mathbf{q}(t) = \mathbf{Q}\exp(-\mathbf{Q}^{-1}\mathbf{R}\mathbf{Q}t)\mathbf{Q}^{-1}\mathbf{q}(0) \quad (12)$$

where $\mathbf{Q}$ is a matrix of eigenvectors of $\mathbf{R}$.

This gives rise to a triple-exponential decay curve for the transverse magnetization with time. Of the three components to the relaxation, the fast component is characteristic of the slow tumbling of the molecule and accounts for about 50% of the magnetization. Two slow components arise from the fast

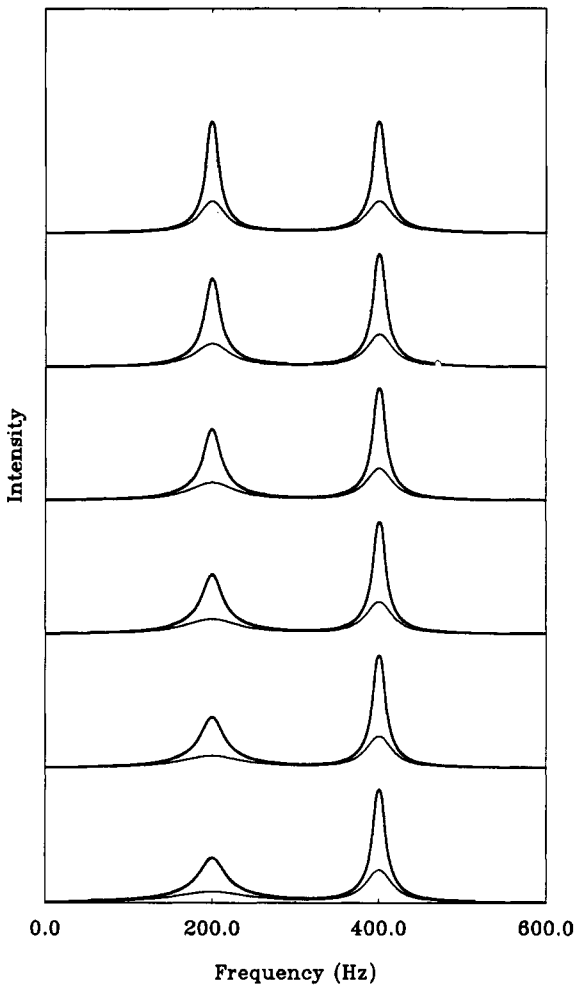

FIGURE 1: Series of simulations of two methyl peaks. The methyl peak at 400 Hz was simulated using an effective correlation time of 10 ns in all the traces. For the methyl peak at 200 Hz, the effective correlation time was varied from 10 ns (top trace) in steps of 4 ns up to 30 ns (bottom trace). The total intensity and the broad component of the peaks are shown in thick and thin lines, respectively.

internal rotation of the methyl group; one of these, however, makes only a very small contribution (≤1%) to the relaxation and was excluded in the analysis of the experimental relaxation data. In the following we assume, therefore, double-exponential relaxation. In these circumstances, a single value of a line width is not meaningful and methyl peaks of 1-D spectra were instead directly simulated for varying effective correlation times. The distance between the methyl protons was set to 1.8 Å (Werbelow & Marshall, 1973); an internal rotational correlation time for the methyl group (τ_{me}) of 0.01 ns and a vicinal coupling constant of 6.7 Hz were used (Li, 1992). The distribution of external protons (i.e., their orientations and distances relative to the methyl group in question) was assumed to be the same for all proteins examined here as for the methyl residues in the triclinic crystal structure of hen egg white lysozyme.

In large macromolecules at high frequency, the fast relaxation component of the spectral line may be so broad that it is effectively submerged into the baseline. The resolved methyl peak will then be dominated by the narrow component and will have an apparent intensity of less than three protons. If, however, there exists an extra degree of fast motional freedom for a part or domain of the molecule, the effective correlation time for that part or domain of the molecule will be shortened. Consequently, the broad component will be narrowed and the intensity will appear to increase. The

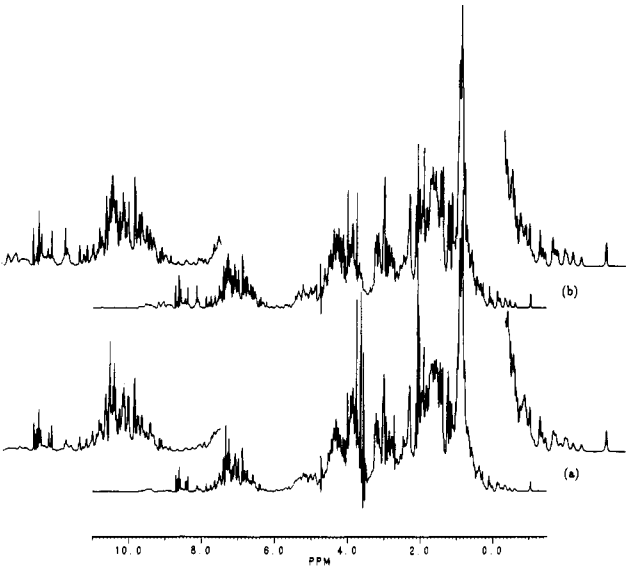

FIGURE 2: 600-MHz 1-D NMR spectra of human urinary (a) and recombinant (b) u-PA at 29 °C, pH 4.5, in D_2O. The insets show expansions of both the low-field and high-field regions of the spectra.

resonances do not, therefore, show as straightforward a dependence of half-height line width on correlation time as do pure Lorentzian lines; this effect is shown in Figure 1.

As a confirmation of the validity of our approach, simulations were performed for lysozyme, a globular protein for which a substantial amount of data is available (Redfield & Dobson, 1988). Simulations for the aromatic tryptophan cross peaks of lysozyme (Trp-28, Trp-63, Trp-108, Trp-123) gave an average line width of 9 ± 1 Hz (at 27 °C), which corresponds to an effective correlation time close to 9.8 ns. The simulation of the methyl peak at –0.66 ppm from Leu-17 of lysozyme in the 1-D spectrum (at 35 °C) gave an effective overall correlation time of 6.0 ns. The apparent discrepancy between the values found here for the methyl protons and for the tryptophan ring protons may be attributed largely to the internal mobility of the side chains which is accounted for by the use of the generalized order parameter S^2 (eq 5). From dynamical simulations of lysozyme, average order parameters S^2 of ca. 0.6 for methyl side chains and 0.8 for tryptophan residues have been found (Olejniczak et al., 1981). Taking these values, the overall correlation time for lysozyme is calculated to be 12.3 ns at 27 °C from simulations of the tryptophan resonances and 10 ns at 35 °C from that of the methyl peaks. These are in good agreement with the experimental value of 10 ± 2 ns at 32 °C for the overall rotational correlation time (τ_c) of the backbone atoms, which has been previously estimated on the basis of a variety of measurements, including light scattering, fluorescence, and ^{13}C T_1 values for backbone C_α atoms (Olejniczak et al., 1981).

RESULTS

The Spectrum of u-PA. Figure 2a shows the spectrum of human urinary u-PA at pH 4.5. The features of this spectrum are very similar to those of spectra reported previously (Bogusky et al., 1989; Oswald et al., 1989), except that the spectral resolution is much improved. In order to optimize spectral resolution, we have explored a wide variety of solution conditions. It was found to be particularly important to work at pH values below 5 and to desalt by means of several cycles through Centricon-3 or -10 cells.

Close inspection of the spectrum of u-PA in Figure 2 shows that it has a large dispersion of chemical shifts, as expected

for a structured globular protein, and that it retains two particularly striking characteristics detected in previous spectra (Oswald et al., 1989). First, the resolved resonances in general appear narrower than expected for a molecule with a molecular mass of 54 kDa, and second, there are at least two sets of peaks characterized by their differing line widths. In the upfield region of the spectrum, peaks attributed to the kringle and the EGF-like domains appear sharper with up to double the apparent intensity of the protease peaks. Because of the complex relaxation behavior of methyl resonances and the possible submerging of the broad component of the peak into the baseline (see Materials and Methods), peaks from methyl protons with longer correlation times will appear to have a lower intensity than the same number of protons of a methyl group with a shorter correlation time. For example (Figure 2a), the most upfield-shifted resonance assigned to the protease domain (at –0.6 ppm) has about half of the apparent intensity of the most upfield-shifted kringle resonance (–1.0 ppm), although both of them represent the three protons of a methyl group. This situation is very similar to that in the middle traces of Figure 1. In the downfield region of the spectrum, there are fewer well-resolved resonances, except for histidine C_2 protons between 8.3 and 8.7 ppm, so that the differential line widths are not as obvious as in the upfield region of the spectrum. Nevertheless, a number of particularly well-resolved resonances can be seen to be present in the spectrum in positions close to those anticipated for kringle resonances (Li et al., 1992).

The spectrum of u-PA has been examined under a range of conditions to explore whether these general features are maintained. Spectra were recorded at pH values from 4 to 7. Because of the lower solubility and the tendency to aggregate at high pH, special care was taken in preparing the samples for this study. The pH of a 0.04 mM sample of human urinary u-PA in D_2O was increased to pH 7.0 prior to a 10-fold concentration step at this pH using Centricon-10 concentration cells. After accumulation of the first spectrum, the pH value was lowered in steps of 0.5 pH units by addition of 0.04% DCl. The results show that the overall features of the spectrum of u-PA are not altered over the pH range studied. In the upfield region, for example, the line widths at higher pH are larger; the relative peak heights of the upfield resonances of the kringle and the protease domain change by approximately 10%, but the characteristic differences between resonances from the kringle and the protease domains are maintained. Changes in chemical shift values of these resolved resonances can be observed, but they are small; the four overlapping resonances between –0.1 and 0.4 ppm at pH 7.0, for example, spread out somewhat at pH 4.0 but do not shift out of this region. In the aromatic region, the most striking feature is the anticipated large change in the spectrum downfield of 8.3 ppm. This can be attributed to the titration of all or most of the 17 histidine residues whose p*K* values fall within this pH range.

Spectra of u-PA were also recorded as a function of the ionic strength of the solution. Starting with a sample at low ionic strength, the salt concentration was raised by adding aliquots of a 2 M NaCl solution, changing the NaCl concentration of the NMR sample from 0 to 180 mM NaCl. At higher concentrations of NaCl, the line widths increase; the effect is not very large and can again be seen most clearly for the resolved resonances at high field. The ratio of apparent intensities of the most upfield-shifted kringle and protease resonances is reduced by only about 5% between 0 and 180 mM NaCl concentration. No differences other than small

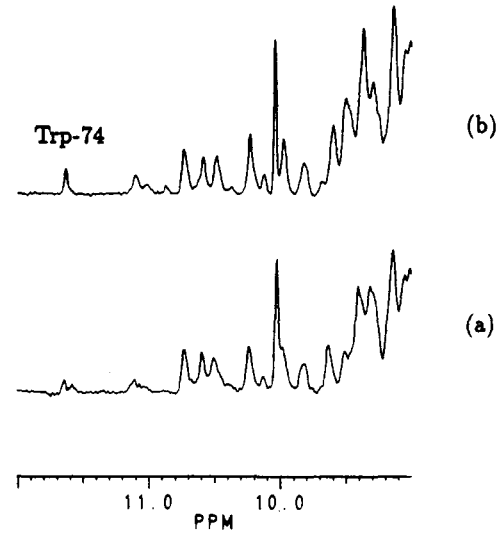

FIGURE 3: Low-field region of the 600-MHz 1-D NMR spectra of human urinary (a) and recombinant (b) u-PA at 35 °C, pH 4.5, in H_2O. The labeled resonance arises from the N(1)H proton of Trp-74(25).

changes in chemical shift positions can be seen in the aromatic region of the spectrum. There is no evidence, therefore, for significant changes in domain structure or interactions over the pH or ionic strength range investigated. The small increases in line width, which are likely to arise from an increased tendency to aggregate at high pH or higher ionic strength (both of which decrease the electrostatic repulsion between molecules) are the origin for the deterioration in spectral quality under these conditions.

In Figure 2b is shown a spectrum of recombinant u-PA. This is virtually identical to the spectrum of human urinary u-PA, although some small differences in chemical shift positions are evident (see, for example, protease resonances in the upfield region between 0.5 and –0.6 ppm in Figure 2b). However, the most significant difference between spectra of human urinary and recombinant u-PA is the better resolution in the latter. The small shifts and improved resolution may be attributed in part to the absence of the carbohydrate moiety which is attached to Asn-302 in the protease domain. Variable fucosylation of the EGF-like domain in native u-PA has also been reported (Buko et al., 1991). The loss of carbohydrate reduces the molecular mass by approximately 8 kDa and will therefore increase the molecular tumbling rate and decrease the line width. The effect of this, however, will be complex because the carbohydrate is heterogenous and likely to be substantially disordered in solution. Indeed, the resonances of the saccharide groups can be seen in the spectrum of human urinary u-PA in Figure 2a; these apparently narrow lines are consistent with extensive motional averaging. That there are other causes for differences between the recombinant and human urinary protein is, however, indicated by the fact that a number of resonances attributed to the kringle domain, which is not glycosylated, appear to differ. The kringle domain from the recombinant protein has been assigned and analyzed in detail. Comparison of the spectrum with that of the isolated human urinary kringle domain shows that many resonances of the latter appear to be split into at least two components. Indeed, this phenomenon can be seen in the spectrum of the intact molecule, most clearly for the resonance of the indole NH proton of Trp-74(25) from the kringle domain (Figure 3) (kringle resonances are referred to by their position in u-PA, consensus kringle numbering starting from Cys-50 as 1 is given in brackets). We believe, therefore, that the human

urinary protein is heterogenous in the kringle domain. In the studies described below only the recombinant protein has been used.

Comparison of Spectra of u-PA and Its Constituent Fragments. Three regions in the DQF COSY spectrum of recombinant u-PA have a chemical shift dispersion large enough to make a detailed analysis possible. These are the region containing cross peaks arising from correlations between methyl groups and their neighboring protons (0.7 to −1.0 ppm), the region resulting from correlations between aromatic protons (5.3–7.9 ppm), and the fingerprint region, containing cross peaks between backbone $C_\alpha H$ and amide NH protons (6–10.5 ppm). In order to analyze the spectrum of u-PA, it was compared with spectra of its domain fragments. The kringle domain has been virtually completely assigned by sequential methods (Li et al., 1992), but no previous information was available for the protease or EGF-like domains. Because of the complexity of the spectrum, resulting from severe spectral overlap, no sequence-specific assignments have been obtained for the protease domain; there are, however, well-resolved cross peaks in all the three regions of the DQF COSY spectrum mentioned above. Eight spin systems could be assigned in the aromatic region of DQF COSY and TOCSY spectra. Because of the high complexity of the spectrum, assignments were confirmed at various temperatures (29, 35, and 50 °C); the spectrum at 50 °C showed particularly good resolution. The two-domain fragment EGF–kringle gives well-resolved spectra and allowed the assignment of a number of resonances in u-PA to the EGF-like domain. As there are only one tryptophan and one tyrosine residue in this domain, sequence-specific assignments were possible for these residues. In the aromatic region and in the upfield region of the spectrum of u-PA, all resolved cross peaks could be classified as originating from one of the three domains. The chemical shift positions in u-PA for all but four resonances are within 0.02 ppm of those in the isolated domains and in intact u-PA and within 0.05 ppm for these four. The isolation of the domains does not, therefore, appear to cause any major structural perturbations.

Figure 4 shows a comparison of the upfield region of the spectrum of u-PA with those from the protease, the EGF-kringle pair, and the kringle domains. Upfield of 0.8 ppm cross peaks from nine spin systems can be assigned to the kringle domain by comparison with the spectrum of the isolated recombinant kringle domain [Leu-96(47), Val-123(74), Lys-61(12), Leu-80(31), Leu-72(23), Val-128(79), Arg-88(39), Val-79(30), and Val-115(66)]. Upfield of 0.02 ppm resonances of some 13 residues can be assigned to the protease domain. One valine could be assigned tentatively to the EGF-like domain, as it is found in the spectrum of EGF–kringle but not in the spectrum of the isolated kringle domain. It could, however, also originate from the interdomain region or from part of the kringle domain, if it were perturbed by the presence of the EGF-like domain. A striking feature of the 2-D spectrum of u-PA is the higher intensity of the cross peaks arising from the kringle and EGF-like domains compared with those of the protease domain; this feature will be commented upon later.

In the aromatic region of the DQF COSY spectrum (Figure 5) in contrast to that of the 1-D spectrum, many kringle resonances can be clearly identified. These include those of Trp-74(25), Trp-112(63), Phe-57(8), Tyr-51(2), Tyr-58(9), Tyr-84(35), and Tyr-101(52) (see Table I). Furthermore, resonances of the only tryptophan (Trp-30) and the only tyrosine (Tyr-24) residues of the EGF-like domain have been identified by comparison with the spectrum of the isolated EGF–kringle domain pair. The identification of the resonances of the two phenylalanine residues of the EGF-like domain and of the two phenylalanine residues of the linker proved to be difficult because of the high degree of overlap in the region of the spectrum between 7.2 and 7.4 ppm, where their resonances are normally found. In the protease domain, resonances of the ring protons of four out of five tryptophan residues, and of two out of nine phenylalanine residues, could be identified. In contrast to the situation for methyl groups, the variation in relative intensities of the resonances of different aromatic residues within a domain is very large and strongly dependent on the type of ring system under investigation. However, when comparing the relative intensities of resonances of the same residue type, the higher intensities of those in the kringle and EGF-like domains are very clear. In the spectrum of the EGF–kringle pair, the higher apparent intensity of resonances from the smaller EGF-like domain is striking.

In the fingerprint region of the DQF COSY spectrum (Figure 6), the variation of intensities of NH–$C_\alpha H$ cross peaks within individual domains is even larger; this can be attributed at least in part to the variation in $J_{NH-C_\alpha H}$ values for different residues. Nevertheless, at least 116 cross peaks can be seen out of the 387 anticipated from the 411 residues of u-PA. In relative terms, far more kringle cross peaks than protease peaks are present in the spectrum, these being identified by comparison with the spectrum of the isolated domains; 40% of the kringle cross peaks (34 out of 85) but only 15% of the protease peaks (39 out of 260) could be clearly identified. A further 15 cross peaks could be identified in the spectrum that are present in the EGF–kringle but not in the kringle or the protease domain. Most of these are likely to originate from the EGF-like domain, but, as mentioned for other regions of the spectrum, some of these could also result from kringle resonances perturbed by the presence of the EGF-like domain.

In the main aliphatic region (1–5 ppm), the spectrum of u-PA has many overlapping cross peaks which make any detailed analysis impossible. There is a subset of very intense cross peaks, which is likely to originate from highly mobile regions of the molecule. At least some of the very intense cross peaks could be from linker residues, although they could also arise from any flexible unstructured part of the molecule, including side chains of surface residues. A comparison with the DQF COSY spectrum of the linker peptide shows, however, no evidence for a set of very narrow resonances arising from the linker residues in u-PA. In a number of other proteins, such residues have been found to give rise to very narrow resonances as a consequence of their extreme flexibility (Perham et al., 1987; Endo & Arata, 1986); this appears not to be the case in u-PA.

Despite the generally poorer resolution in this region of the spectrum, a considerable number of $C_\alpha H$–$C_\beta H$ cross peaks are observed between 4.7 and 5.6 ppm, indicating the existence of a large amount of β-sheet structure in this protein. There are 35 well-resolved $C_\alpha H$–$C_\beta H$ cross peaks, 12 of which can be assigned to the kringle domain, 17 to the protease domain, and 3 to the EGF domain.

Analysis of Line Widths and Effective Correlation Times. In order to analyze the behavior of the different domains, two groups of resonances have been examined in detail. The first is the group of tryptophan cross peaks in the aromatic region of the DQF COSY spectrum, for which the line widths and effective correlation times have been determined. The second is the group of upfield-shifted methyl resonances visible in the 1-D and 2-D spectra. As described earlier, the complex

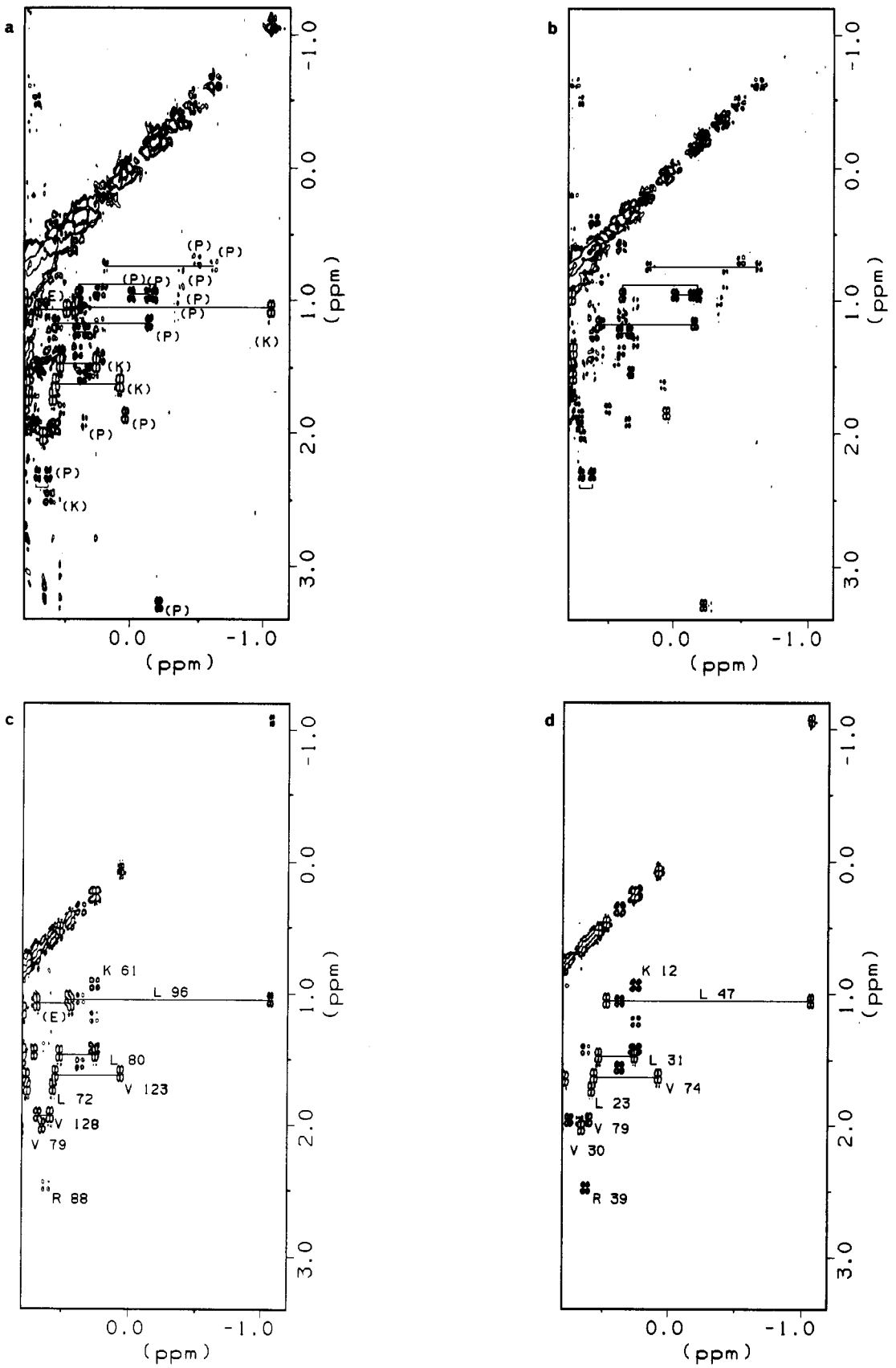

FIGURE 4: Upfield region of the 600-MHz DQF COSY spectra of u-PA (a) and the protease domain (b) at 29 °C, pH 4.5, in D_2O; EGF–kringle (c), and kringle (d) domains at 35 °C, pH 4.5, in H_2O. Cross peaks of the protease, the kringle, and the EGF-like domains are labeled (P), (K), and (E), respectively. Sequence-specific assignments of the kringle domain are numbered according to the u-PA sequence for the spectrum of the EGF-kringle domain pair and according to the consensus kringle sequence for the isolated kringle domain.

relaxation behavior of methyl protons renders the determination of simple half-height line widths meaningless. The effective correlation times and order parameters were therefore used in the simulations of the methyl resonances.

Simulations were performed for residues in the isolated kringle and protease domain and for the same residues within

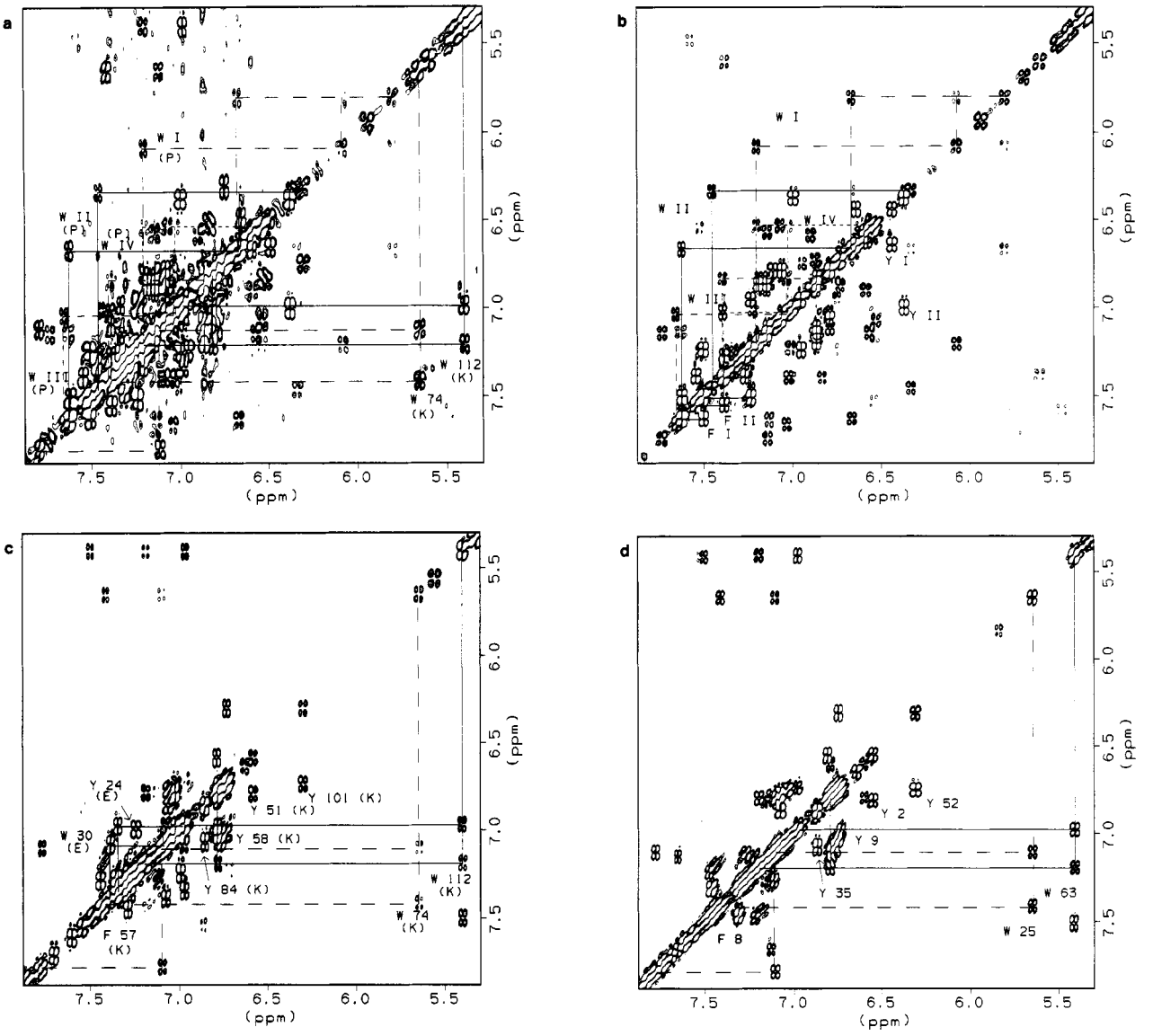

FIGURE 5: Aromatic region of the 600-MHz DQF COSY spectra of u-PA (a) and the protease domain (b) at 29 °C, pH 4.5, and D_2O; EGF-kringle (c) and kringle (d) domains at 35 °C, pH 4.5, in H_2O. Cross peaks of the protease, the kringle, and the EGF-like domains are labeled (P), (K), and (E), respectively. Sequence-specific assignments of the kringle domain are numbered according to the u-PA sequence for the spectrum of u-PA and of the EGF–kringle domain pair and according to the consensus kringle sequence for the isolated kringle domain. In the absence of any sequence-specific assignments for the protease domain, residues from this domain are labeled with Roman numerals.

Table I: Chemical Shifts of Tryptophan, Tyrosine, and Phenylalanine Ring Protons in Recombinant u-PA (ppm) at 29 °C

domain	residue	4H	5H	6H	7H	residue	2,6H	4H	3,5H
EGF	Trp-30	7.40	7.09	6.99	7.34	Tyr-24	7.01		7.26
kringle	Trp-74	7.80	7.12	5.66	7.41	Phe-57	7.32	7.48	7.32
	Trp-112	6.99	5.41	7.21	6.82	Tyr-51	6.54		6.83
						Tyr-58	6.80		7.05
						Tyr-84	6.88		7.09
						Tyr-101	6.32		6.76
protease	Trp-I	7.21	6.09	5.80	6.67	Phe-I	7.24	7.51	7.63
	Trp-II	7.63	6.67	6.34	7.47	Phe-II	7.27	7.39	7.55
	Trp-III	7.67	7.05	6.85	7.39	Tyr-I	6.49		6.67
	Trp-IV	7.40	7.04	6.54	7.21	Tyr-II	6.39		7.01

the intact u-PA. A series of simulations was carried out for the cross peaks of the two tryptophans of the kringle domain (Trp-74 and Trp-112) and for three of the five tryptophans of the protease domain (a total of 12 cross peaks of the spectrum of u-PA, 9 of the isolated protease, and 5 of the isolated kringle domain) and for the seven most upfield-shifted methyl peaks, i.e., the methyl resonance of Leu-96(47) in the kringle domain and six resonances of the protease domain. Neither the tryptophan cross peaks nor the upfield-shifted methyl resonances of the EGF-like domain were well enough resolved to allow simulations to be performed for them. The same was true for one of the four tryptophan residues of the protease domain analyzed in the spectrum of the isolated domain and in the spectrum of the intact protein. Examples of the simulations of tryptophan cross peaks and methyl peaks and comparisons with the corresponding experimental peaks are shown in Figures 7 and 8. The values determined for the line widths were 6 ± 1 Hz and 16 ± 3 Hz for the isolated kringle

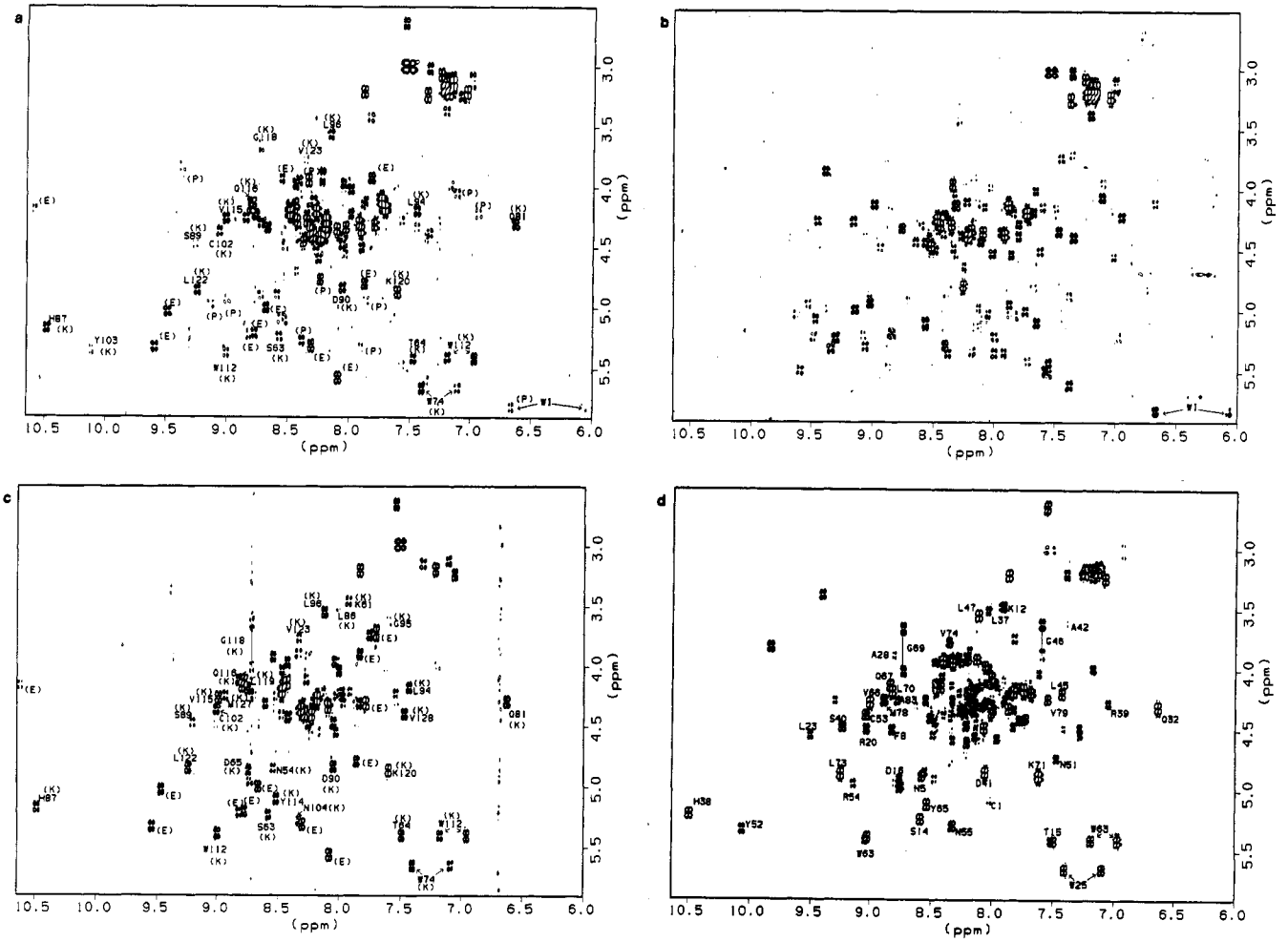

FIGURE 6: Fingerprint region of the 600-MHz DQF COSY spectra of recombinant u-PA (a), the protease domain (b), EGF-kringle (c), and kringle (d) domains at 35 °C, pH 4.5, in H_2O.

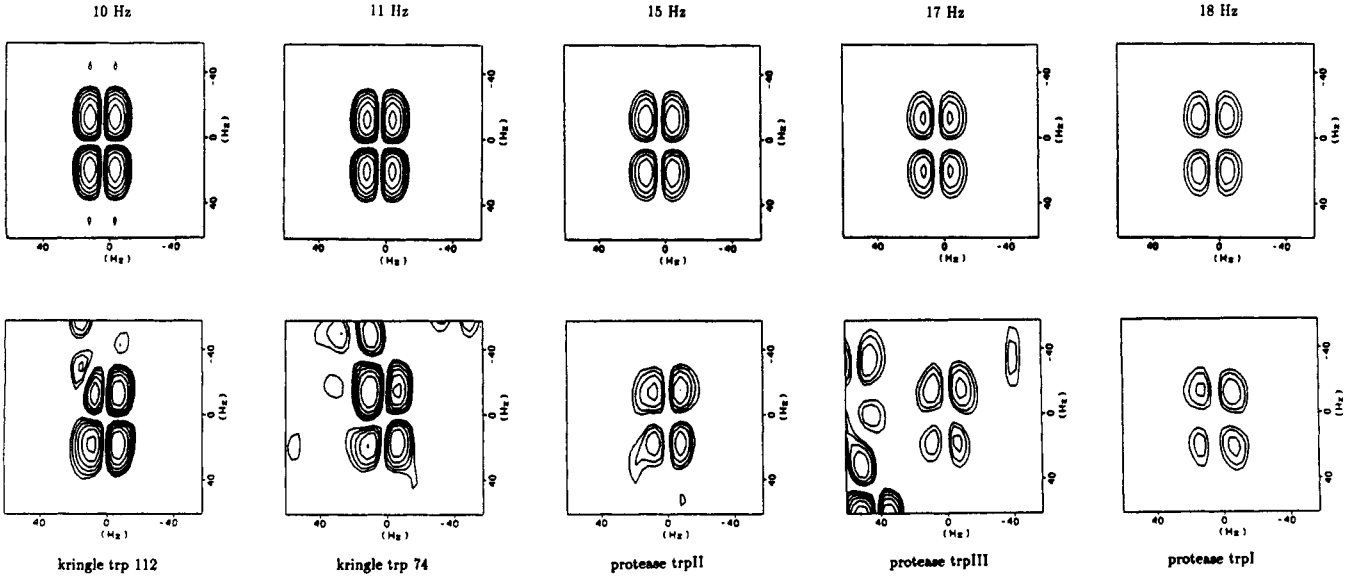

FIGURE 7: Simulations of DQF COSY cross peaks of two tryptophan residues of the kringle domain and three of the protease domain of u-PA in comparison with the experimental cross peaks (cross peaks H5,H4 of the kringle Trp-74 and Trp-112 and of protease Trp-I, Trp-II, and Trp-III). The spectrum was recorded in D_2O, at pH 4.5 and 29 °C. Line width values of 10, 11, 15, 17, and 18 Hz were used for the simulations.

and protease domains, respectively. The corresponding values for the kringle and protease domains within u-PA are 11 ± 2 and 19 ± 3 Hz, respectively. These results yield average effective correlation times of 6.6 and 17.2 ns for the isolated domains and of 12.5 and 20.8 ns for the domains within u-PA. The effective correlation times determined by the best fit of the simulations of the methyl resonances were somewhat smaller, being 5.2 and 12.1 ns for the isolated kringle and protease domains and 9.0 and 15.7 ns for the corresponding domains of intact u-PA (see Table II). The experimental errors in the line width measurements of tryptophan cross peaks translate into errors of between ±1 and ±3 ns in the

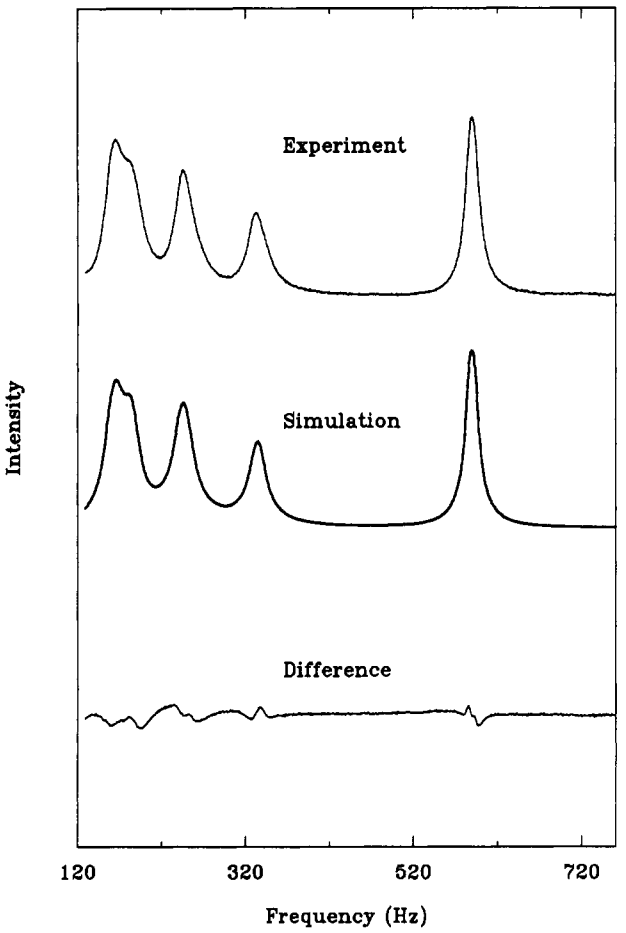

FIGURE 8: Simulation of upfield-shifted methyl peaks in the 600-MHz 1-D NMR spectrum of u-PA. The spectrum was recorded in D_2O at pH 4.5, 29 °C. Effective correlation times of 9.0 ns for the kringle peak (at 600 Hz) and on average 15.7 ± 0.5 ns for the protease peaks were used in the simulations.

Table II: Summary of the Effective Correlation Times (τ_{eff}) and Overall Correlation Times (τ_c) Obtained for Methyl Groups and Tryptophan Residues

	τ_{eff} (ns) methyl	τ_{eff} (ns) tryptophan	τ_c (ns) methyl	τ_c (ns) tryptophan
lysozyme	6.0	9.8	10.0	12.3
kringle (isolated)	5.2	6.6	8.7	8.2
kringle (intact protein)	9.0	12.5	15.0	15.6
protease (isolated)	12.1	17.2	20.2	21.5
protease (intact protein)	15.7	20.8	26.1	26.0

effective correlation times. The corresponding errors in the simulations of the methyl group resonances are hard to estimate reliably, but varying τ_{eff} by ±1 ns from the optimum value gives noticeably poorer fits to the experimental spectra. Some of the differences in the correlation times determined by the two approaches are, therefore, likely to arise not from experimental errors but from the assumptions inherent in an analysis of the type described here. Nevertheless, the values of the effective correlation times are clearly distinct for the different domains within the intact protein, and indeed the relative values of the correlation time estimated by the two methods are very closely similar.

Both tryptophan residues and methyl-containing residues are hydrophobic and are likely to be located in the interior of the protein. Their properties should therefore give a good indication of the mobility of the individual domains in which they are found. However, in order to estimate more accurately the overall domain correlation times (τ_c) involved, the effective correlation times determined were corrected for the different side chain mobility anticipated for these two kinds of residues. This was achieved by applying the order parameter S^2, shown to be appropriate in simulations of lysozyme (see Materials and Methods). These results are shown in Table II. The values of the domain correlation times obtained from analysis of aromatic and methyl resonances are now in extremely good agreement: 15.6 and 15.0 ns for the kringle domain and 26.0 and 26.1 ns for the protease domain in u-PA. This gives confidence in the concept of a uniform overall motion characteristics of each domain and in the conclusion that these differ significantly for the different domains.

DISCUSSION

Our results have demonstrated the importance in any NMR study, and especially in studies of large proteins, of optimizing experimental conditions. These must be conditions under which the solubility is high and the intrinsic line width is minimized; in practice, the best conditions are those that minimize any tendency toward aggregation. Mildly acidic pH was most favorable in the case of u-PA. At pH 4.5, the protein is well below its isoelectric point (pH 8.3) but above the pH values at which domain unfolding begins to be significant at 29 °C. It is likely that aggregation is inhibited by the electrostatic repulsion of the positively charged protein at these relatively low pH values; this is consistent with the observation that resolution is improved at low ionic strength where screening of the charges is minimal.

The second important improvement to earlier studies on u-PA was achieved by studying the recombinant protein instead of the protein of human urinary origin. The improvement in the spectrum is likely to be due in part to the lack of glycosylation in the recombinant protein and the correspondingly reduced molecular weight. We believe, however, that the heterogeneity found in samples of human urinary u-PA and its isolated kringle domain is the main reason for this observation. The core region of the protein, notably Leu-96(47) and Trp-74(25) and Trp-112(63), is, however, found to be identical in the two samples, as seen by the closely similar chemical shifts for these residues. The origin of the heterogeneity is, therefore, not yet clear.

At a very early stage of the studies on u-PA, it became evident that spectra of the quality achieved for this protein could only be possible if there exists segmental motion additional to the overall tumbling of the protein. From the known domain structure of u-PA, it appeared most likely that, at the very least, the linker between the kringle and the protease domain allows some independence of motion between these two domains (Oswald et al., 1989). Further evidence for the independence of the domains has come from the finding from NMR (Bogusky et al., 1989) and recently differential scanning calorimetry studies (DSC) (Novokhatny et al., 1992) that the domains of u-PA unfold in an autonomous manner during thermal denaturation.

The present study shows that substantial independent domain motion does indeed exist and that it is maintained over a wide range of pH and ionic strength. Although the kringle resonances broaden somewhat more markedly than protease resonances, there is still a substantial difference in line width between these two sets of resonances at pH 7.0. This shows that independent motion of the kringle and the protease domains in u-PA persists under conditions closer to physiological than those ideal for detailed NMR experiments.

The overall broadening implies some small increase in intermolecular interactions at higher pH or higher ionic strength, but because of the high protein concentrations used in NMR experiments, these aggregation effects are not in themselves of physiological relevance. The small changes in the differential line widths of the kringle and the protease resonances could result either from this or from intramolecular effects arising from slightly closer contacts and reduced flexibility between the two domains. The relatively small influence of the pH and salt concentration on the interaction of the domains of u-PA is in contrast to studies on miniplasminogen, a two-domain fragment of plasminogen comprising the protease domain and kringle 5, spectra of which proved to be very sensitive to changes in the pH and ionic strength of the samples (Teuten, 1991).

Whereas the differential mobility of the kringle and the protease domains is revealed in the 1-D studies by the higher apparent intensity of the resolved upfield-shifted methyl peaks from the former domain, this behavior also shows itself in the 2-D spectra by the difference of cross peak intensities of the aromatic resonances from the two domains. For large macromolecules, as the line width increases, the overlap of antiphase lines causes a partial cancellation and reduction of the cross peak intensity. Many factors may influence the line width of a resonance. They include the overall tumbling of the molecule, which is proportional to the molecular weight for a spherical particle and is characterized by the rotational correlation time, and any additional mobility within the molecule such as domain motion, the flexibility of surface loops, and the motions of individual side chains. The intensities of cross peaks are further complicated by variations in coupling constants. Whereas these can be thought of as constant for identical protons of aromatic rings or methyl groups, the intensities of NH–C_αH cross peaks in the fingerprint region are influenced by NH–C_αH coupling constants, which depend on ϕ angles, and by C_αH–C_βH coupling constants, which depend on χ_1 angles.

The series of simulations performed for tryptophan 2-D cross peaks in the aromatic region and the 1-D peaks of the methyl groups in the upfield region of the spectrum was designed to study the segmental mobility in u-PA in greater detail. Especially in the aromatic region, large differences in intensity can be seen for resonances from different residues within one domain. This may be attributed at least in part to additional mobility through flipping of the aromatic rings of tyrosine and phenylalanine residues and to the greater freedom of motion of surface residues compared to internal residues. For this reason, identical spin systems within different domains were examined to explore the domain mobility rather than local motions. The bulky tryptophan residues, which are not subject to ring flips and are normally located in hydrophobic cores of proteins, are especially feasible for this study. Even for these and for methyl-containing residues in the protein core, side chain mobility will contribute motion additional to the overall tumbling and will therefore narrow the resonance lines. A general order parameter S^2 (Lipari & Szabo, 1982) was used to account for these internal motions. The fact that the different residues of both types in each domain when corrected for S^2 values predicted in theoretical simulations gave highly consistent results suggests strongly that the approach we have adopted is valid and that the different domains do indeed have well-defined and distinct motional correlation times. That the behavior of various residues in each domain is similar indicates that the assumption of isotropic motion for the domains, which we have made here, is also reasonable.

The measurement of these correlation times enables us to examine different models for the dynamics of u-PA. If the kringle and protease domains were to be closely associated, the two domains would tumble together and have the same overall correlation time, i.e., the ratio of the measured correlation times would be 1:1. On the other hand, if the domains were fully independent, the ratio would, according to the Stokes–Einstein equation, be approximately equal to the ratio of their molecular weights. One complication for the u-PA analysis is the fact that it is not clear how closely the EGF-like domain is associated with the kringle domain. The spectral simulations could not be extended to this domain, because there are no resolved methyl resonances in the 1-D spectrum and the only tryptophan spin system shows large spectral overlap with other cross peaks in the aromatic region. Therefore we must examine two cases. In the first, the EGF-like domain is assumed to be closely associated with the kringle domain; in this case the ratio of the total molecular weights of these two domains to that of the protease domain would be 1:2.0. In the second case, the motion of the kringle domain is assumed to be totally unconstrained by the presence of the EGF-like domain. In this case the ratio of the correlation times of residues in the kringle and protease domain is in the simplest case the ratio of their individual molecular weights, i.e., 1:3.0.

Our results indicate that the ratio of correlation times for the kringle and the protease domains is 1:1.7, i.e., closer to 1:20 than to 1:30 (Table II, see also Figure 1). The experimental ratio would be consistent, within experimental errors, with a model in which the kringle and the protease domains are not tightly associated, i.e., there is substantial motional independence between these two domains, but the EGF-like domain has strong interactions with the kringle domain. It is necessary, however, to consider the possibility that the degree of independence of the different domains is intermediate between total freedom and total association. Our experimental ratio of correlation times would, for example, be consistent with a model in which the EGF-like and the kringle domains are not highly correlated, but the freedom of motion about the linker between the kringle and the protease domains, while still substantial, is restricted to a certain degree. Both models indicate clearly that there is a high degree of motional freedom between the kringle and the protease domains, but that the second model is more probable is suggested by the fact that τ_c is considerably larger for the kringle domain in intact u-PA than for the isolated kringle molecule (Table II); this suggests that in the intact molecule the motion of the kringle domain is hindered by the presence of the protease domain. Similarly, τ_c for the protease domain is larger in u-PA than in the isolated domain. The difference is much smaller than for the kringle domain, but this is expected since the protease domain is larger than the kringle domain and so the effect of restricted domain mobility will be smaller. Further support for this model comes from the spectrum of the isolated EGF–kringle pair. Although resonances of the tryptophan in the EGF-like domain could not be analyzed quantitatively, they appear to have somewhat higher apparent intensity in the spectrum of EGF-kringle, and of u-PA, than the kringle resonances (Figure 5), implying that their line widths are less and the effective correlation times of their residues are shorter. Further studies are, however, needed to confirm this result.

The motional independence between at least two and probably all three of the domains in u-PA is likely to be of

major functional importance. It implies a disconnection of the domains responsible for binding or recognition processes, the EGF-like and kringle domains, from the catalytic part of the molecule, the protease domain. This might be of considerable value in enabling the different regions of the protein to locate their binding partners. These partners (receptor, plasminogen, and possibly extracellular matrix polysaccharide) are themselves complex macromolecules. Thus, such motional independence provides a means of overcoming the complex topological problem that might exist if the different regions of the molecule were to be rigidly located relative to one another. More particularly, NMR studies of plasminogen and t-PA, while less detailed than those described here for u-PA, provide clear evidence that at least some degree of domain independence is also a feature of these proteins (Teuten, 1991; Teuten et al., 1991). Our NMR results add to the mounting experimental evidence that domain mobility, and the consequent separation of functionally distinct regions, might be a common feature of proteins involved in fibrinolysis and indeed of other multidomain proteins.

ACKNOWLEDGMENT

We are grateful to Grünenthal GmbH, Germany, Delta Biotechnology Ltd., U.K., and the Japan Chemical Research Co. Ltd., Japan for providing protein samples. We thank Maureen Pitkeathly for synthesizing the linker peptide, Christina Redfield for providing the program for 2-D simulations, and Derek Saunders for many valuable discussions.

REFERENCES

Appella, E., Robinson, E. A., Ullrich, S. J., Stopelli, M. P., Corti, A., Cassani, G., & Blasi, F. (1987) *J. Biol. Chem. 262*, 4437–4440.

Bax, A., & Davis, D. G (1985) *J. Magn. Reson. 65*, 355–360.

Blasi, F. (1988) *Fibrinolysis 2*, 73–84.

Bogusky, M. J., Dobson, C. M., & Smith, R. A. G. (1989) *Biochemistry 28*, 6728–6735.

Braunschweiler, L., & Ernst, R. R. (1983) *J. Magn. Reson. 53*, 512–528.

Buko, A. M., Kentzer, E. J., Petros, A. M., Menon, G., Ziuderweg, E. R. P., & Sarin, V. K. (1991) *Proc. Natl. Acad. Sci. U.S.A. 88*, 3992–3996.

Byeon, I. L., & Llinás, M. (1991) *J. Mol. Biol. 222*, 1035–1051.

Byeon, I. L., Kelley, R. F., & Llinás, M. (1991) *Eur. J. Biochem. 197*, 155–165.

Dano, K., Andreasen, P. A., Grondahl-Hansen, J., Kristensen, P., Nielsen, L. S., & Shriver, L. (1985) *Adv. Cancer Res. 44*, 140–266.

Davis, D. G., & Bax, A. (1985) *J. Am. Chem. Soc. 107*, 2820–2821.

de Munk, G. A. W., & Rijken, D. C. (1990) *Fibrinolysis 4*, 1–9.

de Vos, A. M., Ultsch, M. H., Kelley, R. F., Padmanabhan, K., Tulinsky, A., Westbrook, M. L., & Kossiakoff, A. A. (1992) *Biochemistry 31*, 270–279.

Endo, S., & Arata, Y. (1985) *Biochemistry 24*, 1561–1568.

Gilbert, W. (1978) *Nature 271*, 501–502.

Günzler, W. A., Henninger, W., Hennies, H. H., Ötting, F., Scheider, J., Friderichs, E., Giertz, H., Flohé, L., Blaber, M., & Winkler, M. (1984) *Haemostasis 14*, 60.

Gurewich, V., Pannell, R., Louie, S., Kelley, P., Suddith, R. L., & Greenlee, R. (1984) *J. Clin. Invest. 73*, 1731–1739.

Gurewich, V., Pannell, R., Broeze, R. J., & Mao, J.-I. (1988) *J. Clin. Invest. 82*, 1956–1962.

Handoll, H. G. (1985) D. Phil. Thesis, University of Oxford.

Holmes, W. E., Pennica, D., Blaber, M., Rey, M. W., Günzler, W. A., Steffens, G. J., & Heyneker, H. L. (1985) *Biotechnology 3*, 923–929.

Hubbard, P. S. (1958a) *Phys. Rev. 109*, 1153–1158.

Hubbard, P. S. (1958b) *Phys. Rev. 111*, 1746–1747.

Hubbard, P. S. (1969) *J. Chem. Phys. 51*, 1647–1651.

Li, X. (1992) D. Phil. Thesis, University of Oxford.

Li, X., Smith, R. A. G., & Dobson, C. M. (1992) *Biochemistry 31*, 9562–9571.

Lijnen, H. R., Van Hoef, B., & Collen, D. (1987) *Eur. J. Biochem. 162*, 351–356.

Lijnen, H. R., Van Hoef, B., Nelles, L., & Collen, D. (1990) *J. Biol. Chem. 265*, 5232–5236.

Lipari, G., & Szabo, A. (1982) *J. Am. Chem. Soc. 104*, 4546–4559.

Mangel, W. F., Lin, B., & Ramakrishnan, V. (1991) *J. Biol. Chem. 266*, 9408–9412.

Mazar, A. P., Buko, A. M., Petros, A. M., Barnathan, E. S., & Henkin, J. (1992) *Fibrinolysis 6 (Suppl. 1)*, 49–55.

Mulichak, A. M., Tulinsky, A., & Ravichandran, K. G. (1991) *Biochemistry 30*, 10576–10588.

Novokhatny, V., Medved, L., Mazar, A., Marcotte, P., Henkin, J., & Ingham, K. (1992) *J. Biol. Chem. 267*, 3878–3885.

Olejniczak, E. T., Poulsen, F. M., & Dobson, C. M. (1981) *J. Am. Chem. Soc. 103*, 6574–6580.

Oswald, R. E., Bogusky, M. J., Bamberger, M., Smith, R. A. G., & Dobson, C. M. (1989) *Nature 337*, 579–582.

Park, C. H., & Tulinsky, A. (1986) *Biochemistry 25*, 3977–3982.

Patthy, L. (1985) *Cell 41*, 657–663.

Perham, R. N., Packman, L. C., & Radford, S. E. (1987) *Biochem. Soc. Symp. 54*, 67–81.

Rance, M., Sorensen, O. W., Bodenhausen, G., Wagner, G., Ernst, R. R., & Wüthrich, K. (1983) *Biochem. Biophys. Res. Commun. 117*, 479–485.

Redfield, A. G. (1965) *Adv. Magn. Reson. 1*, 1–32.

Redfield, C. (1984) Ph.D. Thesis, Harvard University, Cambridge, MA.

Redfield, C., & Dobson, C. M. (1988) *Biochemistry 27*, 122–136.

Reilly, D., Andreasen, P. A., & Duffy, M. J. (1991) *Blood Coagulation Fibrinolysis 2*, 47–50.

Steffens, G. J., Günzler, W. A., Ötting, F., Frankus, E., & Flohé, L. (1982) *Hoppe-Seyler's, Z. Physiol. Chem. 363*, 1043–1058.

Stephens, R. W., Bokman, A. M., Myöhänen, H. T., Reisberg, T., Tapiovaara, H., Pedersen, N., Grondahl-Hansen, J., Llinás, M., & Vaheri, A. (1992) *Biochemistry 31*, 7572–7579.

Teuten, A. J. (1991) D. Phil. Thesis, University of Oxford.

Teuten, A. J., Smith, R. A. G., & Dobson, C. M. (1991) *FEBS Lett. 278*, 17–22.

Tropp, J. (1980) *J. Chem. Phys. 72*, 6035–6043.

Tulinsky, A., Park, C. H., & Skrzypczak-Jankun, E. (1988) *J. Mol. Biol. 202*, 885–901.

Werbelow, L. G., & Marshall, A. G. (1973) *J. Magn. Reson. 11*, 299–313.

Werbelow, L. G., & Grant, D. M. (1977) *Adv. Magn. Reson. 9*, 189–299.

Winkler, M. E., & Blaber, M. (1986) *Biochemistry 25*, 4041–4045.

Winkler, M. E., Blaber, M., Bennett, G. L., Holmes, W., & Vehar, G. A. (1985) *Biotechnology 3*, 990–1000.

Wu, T. P., Padmanabhan, K., Tulinsky, A., & Mulichak, A. M. (1991) *Biochemistry 30*, 10589–10594.